CHAPTER VI
FORMATION OF NANOCRYSTALLINE ZnO ON NANOFIBRIALS OF BACTERIAL CELLULOSE PELLICLE BY IN SITU SYNTHESIS UNDER ULTRASONIC TREATMENT

6.1 Abstract

In this study, the nanocrystalline zinc oxide (ZnO) particles were successfully synthesized and simultaneously incorporated into the nanofibrous matrix of bacterial cellulose (BC) by using the ultrasonic assisted-*in situ* synthesis method. The new proposed-preparation method was composed of the two step-wised immersion methods. BC pellicle was firstly immersed in zinc acetate solution. Then, the Zn^{2+} absorbed-BC pellicle was immersed in ammonium hydroxide solution with simultaneously ultrasonic treating. The synthesis route and the growth mechanism of ZnO crystal on the nanofibrous BC were firstly proposed in this study. The formation of nanocrystalline ZnO particles inside the BC were investigated by the scanning electron microscope (SEM) with inbuilt of the energy dispersive X-ray analysis (EDX). The crystalline structure and crystalline size of ZnO particles were examined by the X-ray diffraction (XRD). The crystalline size of ZnO particles was calculated to be 53.83–63.25 nm. Interestingly, the crystalline size of ZnO particles was corresponded to the diameter of the BC; the diameter of the BC was 44.46–65.54 nm. By the aid of ultrasonic treatment, ZnO crystal was forced to growth on the surface of the nanofibrous BC. Therefore, the nanofibrous BC surface might be acted as the nucleating surface for the growth of ZnO crystal which resulted in the formation of the nanocrystal ZnO. Percent incorporation of nanocrystalline ZnO particles inside the BC was determined by thermogravimetric analysis (TGA). The percent incorporation of nanocrystalline ZnO particles was increased from 36.82 to 44.77 wt% with increasing the immersion time of BC pellicle in zinc acetate solution from 1 to 3 h. Then, the percent incorporation of nanocrystalline ZnO particles was reached to the equilibrium at 45.93 wt% with 6 h of the immersion time. Even at the equilibrium amount of the incorporated-ZnO particle (45.93 wt%), the structure of the as-prepared nanocrystalline ZnO particle incorporated-BC was still retained in

control the crystalline size of the ZnO particles and provide high porosity structure for allowing the target species to react with nanocrystalline ZnO particles. Finally, the unique properties of nanocrystalline ZnO inside the as-prepared nanocrystalline ZnO particle incorporated-BC was represented by the antibacterial test against *Escherichia coli* (Gram negative) and *Staphylococcus aureus* (Gram positive).

6.2 Introduction

Zinc Oxide (ZnO) is an important and attractive inorganic semiconductor since it exhibits wide band gap (3.37 eV) and large exciton-binding energy (60 meV) (Applerot, Perkas, Amirian, Girshevitz, & Gedanken, 2009). These unique characteristics of ZnO leading to a wide range of technological applications such as luminescence, photocatalyst, piezoelectric transducer, actuators, gas sensors and solar cells (Sulieman, Huang, Liu, & Tang, 2007; An, Cao, & Zhu, 2007; Li, Fang, Liu, Ren, Huang, & Zhao, 2008; Wu, Wu, & Lü, 2006; Liu, Huang, Li, Duan, & Ai, 2006; Cao, Lan, Zhao, Shen, & Yao, 2008; Jia, Yue, Zheng, & Xu, 2008). Recently, ZnO was received more and more attention on their nanoscale properties. Due to their small sizes and large surface-to-volume ratios which have superior properties compared to their bulk counterparts, they are promising candidates for novel nanoscale electronic, optical and mechanical devices (Hu, Chen, Zhou, & Wang, 2010). Moreover, the high specific surface area due to the reducing in particle size into micrometer or nanometer scale was also resulted in the antibacterial properties of ZnO particles (Jung, Oh, Lee, Yang, Park, Park, & Jeong, 2008). The antibacterial property of ZnO particles strongly depends on their size. With the smaller size of crystalline, it will have more efficient in antibacterial activity (Applerot, Lipovsky, Dror, Perkas, Nitzan, Lubart, & Gedanken, 2009). Due to many advantages of nanoscale ZnO, various methods have been employed to achieve ZnO with desired size and morphology such as sol-gel method (Lee, Ko, & Park, 2003), vapor deposition (Wu & Liu, 2002), precipitation (Wang & Muhammed, 1999), thermal decomposition (Casavola, Buonsanti, Caputo & Cozzoli, 2008), hydrothermal synthesis (Sue, Kimura, & Arai, 2004) and spray pyrolysis (Tani, Madler, & Pratsinis. 2002). However, the nanoscale ZnO still had limitations due to the

extremely high surface area. The dispersion of ZnO nanoparticles in polymers or organic matrices was very difficult. There were always agglomerated to be a large particle with the lack of desired-properties.

Recently, the ultrasonic-assisted synthesis method or sonochemical synthesis process has been proposed as an effective method for synthesizing and simultaneously coating of micro or nanoparticle ZnO into the matrix. This method was performed by synthesizing of ZnO particles with the aid of ultrasonic treatment. The chemical activation of the ultrasonic-assisted synthesis method is provided through the energy from cavitations bubble collapse. By providing the ultrasonic treatment, the formation, growth, and implosive collapse of bubbles are continuously occurred in a liquid medium. The rapid collapse of cavitations bubbles generates extremely high temperature (>5000 K), pressure (>200 MPa), and cooling rate (>10^7 K/s) (Suslick, Choe, Cichowlas, & Grinstaff, 1991; Didenko & Suslick, 2002). These extreme conditions could reduce the diameter of ZnO particles into micrometer or nanometer scale (Applerot, Lipovsky, Dror, Perkas, Nitzan, Lubart, & Gedanken, 2009). Many researchers have been reported that the ultrasonic-assisted synthesis method was an effective process for coating of the micro- or nano-scale ZnO on various kinds of substrate such as mesoporous ceramics, polymer supports, fabrics, and glasses (Kotlyar, Perkas, Amiryan, Meyer, Zimmermann, & Gedanken, 2007; Pol, Srivastava, Palchik, Palchik, Slifkin, Weiss, & Gedanken, 2002; Pol, Wildermuth, Felsche, Gedanken, & Calderon-Moreno, 2005).

Among several of kinds of porous substrate, bacterial cellulose (BC) was very attractive and interesting. BC is high purified nanofibrous cellulose produced from the metabolism process of *Acetobacter xylinum* (*A. xylinum*) bacteria by using glucose as a carbon source. BC is produced in the form of multilayer structure of three-dimensional nonwoven network of nanofibrous cellulose. Basically, BC has the same chemical structure as vascular plant cellulose, linear α–1,4–glucan chains (Czaja, Romanovicz, & Malcolm Brown, 2004) but the physical structure of the BC is totally different from the vascular plant cellulose. The three-dimensional structure was found only in the BC but not in the vascular plant cellulose (Rezaee, Solimani, & Forozandemogadam, 2005; Wan, Hong, Jia, Huang, Zhu, Wang, & Jiang, 2006; Grzegorczyn & Ezak, 2007). This structure of BC resulted in high cellulose

crystallinity (60–80%) and as high Young's modulus of 138 GPa and tensile strength of at least 2 GPa, which are almost equal to those of aramid fibers (Li, Chen, Hu, Shi, Shen, Zhang, & Wang, 2009). The nanometer scale diameter of BC fiber, about 100 times smaller than fibrils in plant cellulose, leads to a large surface area that can hold large amount of water (up to 200 times of its dry mass) and display a great elasticity and a high wet strength. (Klemm, Schumann, Udhardt, & Marsch, 2001; Czaja, Young, Kawecki & Brown, 2007). One of the most important features of BC is its chemical purity. BC is free of lignin and hemicelluloses, whereas plant cellulose usually associates with these chemicals. Furthermore, the high chemical purity and high liquid absorption capacity resulted in a good biocompatibility of BC. These unique physical properties, mechanical properties, and chemical purity of BC leading to wide range of applications such as paper industrial, headphone membranes, food industrial (Li, Chen, Hu, Shi, Shen, Zhang, & Wang, 2009), biomaterials including temporary skin substitute, artificial blood vessels (Czaja, Young, Kawecki, & Brown, 2007; Kamel, 2007) and membrane for pervaporation of water-ethanol binary mixtures (Dubey, Saxena, Singh, Ramana & Chauhan, 2002). Moreover, BC also serves as an applicable matrix for impregnating of nanoparticles or nanowires such as cadmium sulfide nanoparticles (Li, Chen, Hu, Shi, Shen, Zhang, & Wang, 2009), silver chloride nanoparticles (Hu, Chen, Li, Shi, Shen, Zhang, & Wang, 2009), silver nanoparticles (Maneerung, Tokura, & Rujiravanit, 2008) and titania nanowires (Zhang & Qi, 2005).

According to several advantages of BC, the BC was expected to be a promising matrix for ZnO particle. In this study, BC was utilized as a template for synthesizing of the ZnO particles with the aid of ultrasonic treatment. The formation of ZnO crystal as well as the growth of ZnO particles inside the BC matrix was investigated. Generally, the ultrasonic-assisted synthesis method was aimed for coating the ZnO particles onto the surface of substrate. In order to direct the ZnO particles to grow inside the BC matrix, the ultrasonic-assisted synthesis method was developed by using the concept of *in situ* synthesis method; the precursor was firstly mixed or incorporated into an organic matrix then crystallization of such particles were performed inside an organic matrix. By using the *in situ* synthesis concept, the ultrasonic-assisted *in situ* synthesis method was performed by immersing the BC

pellicle into zinc acetate solution until the pellicle was saturated with Zn^{2+} and the absorbed Zn^{2+} was converted to ZnO particles inside the BC matrix. The nucleation and growth of ZnO crystal on the nanofibrous cellulose as well as the formation of the ZnO particles inside the BC matrix were firstly investigated in this study. Moreover, the antibacterial activity of the nanocrystalline ZnO particle incorporated-BC was tested against *Escherichia coli* (*E. coli*, Gram negative bacteria) and *Staphylococcus aureus* (*S. aureus*, Gram positive bacteria). The antibacterial activity of the as-prepared nanocrystalline ZnO particle incorporated-BC was evidenced to confirm the reactivity of the incorporated-ZnO particles presenting in the BC matrix.

6.3 Experimental

6.3.1 Materials

Acetobacter xylinum (strain TISTR 975), an isolated strain in Thailand, was supplied from the Microbiological Resources Centre, Thailand Institute of Scientific and Technological Research (TISTR). Analytical grade anhydrous of D-glucose was obtained from Ajax Finechem. Bacteriological grade of yeast extract powder was purchased from HiMedia. Analytical grade of zinc acetate dihydrate was purchased from Ajax Finechem. Other chemical reagents used in this study were analytical grade and used without further purification.

6.3.2 Production of bacterial cellulose

The production of the BC was performed by a partial modification of the method developed by Maneerung, Tokura, and Rujiravanit (2008).

Pre-inocula for all experiments were prepared by transferring a single colony of *A. xylinum* bacteria into 20 ml of a liquid culture medium, which was composed of 40 g of anhydrous D-glucose, 10 g of yeast extract powder, and 1 l of distilled water. The medium composes of 4 g D-glucose anhydrous and 1 g yeast extract powder. After 24 h of cultivation at 30°C, 2.5 ml of the cell suspension was introduced into a 200 ml-Erlenmeyer flask containing 25 ml of fresh liquid culture medium and then cultivated at 30°C for 4 days. The obtained BC was purified by boiling in 1 % NaOH solution for 2 h. The boiling step was repeated twice. The

purified BC was then treated with 1.5 % acetic acid for 30 min, and finally washed in a tap water until BC pellicles became neutral. Porous structure of the BC was preserved by immersing the BC pellicle in distilled water and kept it in a refrigerator at 4°C prior to use.

6.3.3 The preparation of ZnO particle incorporated-bacterial cellulose by ultrasonic-assisted in situ synthesis method

Zinc acetate dihydrate ($Zn(CH_2COO)_2 \cdot 2H_2O$) was used as a precursor. About 0.1 moles (21.95 g) of zinc acetate dihydrate was dissolved in 200 ml of water-ethanol (1:9) mixture prior to keep under vigorously stirring at 50°C. After the dissolution complete, a BC pellicle was immersed in zinc acetate solution for a fixed period of time (1, 3 and 6 h.). Then, the Zn^{2+} absorbed-BC was immersed in 200 ml of ammonium hydroxide solution (pH 8) equipped with a high-intensity ultrasonic bath (Branson sonicator 2510; 40 kHz) and the ultrasonic treatment was immediately done for a fixed period of time. The sonication time was varied to be 0.5, 1 and 2 h for each experiment. After treating with ultrasonic, the as-prepared BC pellicle was washed against large amount of distilled water and then resonicated for 30 min in order to remove any loosely bound nanoparticles. Finally, the obtained samples were freeze-dried and kept in desiccators.

6.3.4 Characterization

The morphology of the neat and magnetic particle-incorporated bacterial cellulose sheets were observed by using a JEOL JSM-5200 scanning electron microscope with inbuilt energy dispersive X-ray analysis (EDX) with operating condition at 15 kV and magnification of 10,000x. The formation of magnetic particles was verified by X-ray diffraction (XRD) (Rigaku). The samples were scanned from $2\theta = 10°$ to $2\theta = 70°$ at a scanning rate of 5° 2θ/min. Thermogravimetric analyser (Perkin Elmer model TGA7) was used to record the thermograms in the temperature range from 50 to 700 °C with a heating rate of 10 °C/min in a flow of nitrogen at 20 ml/min. Transmission electron microscopy (TEM) observations were carried out on a JEOL JEM-2000EX instrument operated at accelerating voltage of 80 kv. The TEM samples were prepared by embedding the

freeze dried bacterial cellulose in Spurr resin and performing ultrathin sectioning with a Reichert Ultracut E microtome equipped with a diamond knife. Histograms, average diameters and standard deviations were obtained by sampling 200 metal nanoparticles in TEM images of 100,000x magnification.

Morphology of the neat BC and the ZnO particle incorporated-BC was investigated by using the JEOL JSM-5200 scanning electron microscope (SEM) with inbuilt energy dispersive X-ray analysis (EDX). The SEM and EDX images of ZnO particle incorporated-BC could be roughly examined the structure of the ZnO particle inside the as-prepared ZnO particle incorporated-BC sample. The crystal structure and the crystalline size of ZnO particles inside the as-prepared ZnO particle incorporated-BC sample were studied by X-ray diffraction (XRD) (Rigaku). The as-prepared ZnO particle incorporated-BC samples were scanned from $2\theta = 20°$ to $2\theta = 80°$ at a scanning rate of 5° 2θ/min. The crystalline size (D) of ZnO particles inside the as-prepared ZnO particle incorporated-BC sample was calculated by the Debye-Scherrer formula,

$$D = 0.89\lambda/\beta \cos\theta$$

where λ is the wavelength of X-rays (λ = 0.15418 nm), β is the full width in radians at half-maximum of diffraction peaks (the peak at $2\theta = 36.3°$ was adopted according to Hirai and Asada (2005)), and θ is the Bragg angle of the XRD pattern. Thermal stability of the as-prepared ZnO particle incorporated-BC sample and percent incorporation of ZnO particles inside the as-prepared ZnO particle incorporated-BC sample were studied by using thermogravimetric analysis (TGA, Perkin Elmer TGA7). Thermograms of the as-prepared ZnO particle incorporated-BC sample was in the temperature range from 50 to 750 °C with heating rate of 10 °C/min in a flow of air at 20 ml/min.

6.3.5 Antibacterial activity studies

Antibacterial activities of neat BC and the as-prepared ZnO particle incorporated-BC sample were studied against *Escherichia coli* (*E. coli*, Gram negative bacteria) and *Staphylococcus aureus* (*S. aureus*, Gram positive bacteria). According to the literature, ZnO particle exhibited difference antibacterial activity against Gram-positive and Gram-negative bacteria. Hence, the antibacterial activity

of the as-prepared nanocrystalline ZnO particle incorporated-BC sample was studied by the disc diffusion method and the colony forming count method for a qualitative and quantitative method, respectively.

6.3.5.1 The disc diffusion method

This method was performed in Luria-Bertani (LB) medium solid agar Petri dish. The neat BC and the as-prepared ZnO particle incorporated-BC samples were cut into a disc shape with 1 cm diameter, sterilized by UV light and placed on *S. aureus*- and *E. coli*-cultured agar plates which were then incubated for 24 h at 37°C. After 24 h of incubation, the inhibition ring was visualized around the samples. The results were reported in term of thickness of the inhibition ring.

6.3.5.2 The colony forming count method

In order to determine the assay of tested bacteria, each bacterium was inoculated on the fresh LB agar plates at 37°C for overnight. After that, one loop of each bacterium was inoculated to each sterilized culture test tube containing 5 ml of LB medium and incubated in an incubator at 37°C overnight. The resultant culture of *S. aureus* and *E. coli* had cell concentration of 10^7 bacteria/ml of culture medium. These cell suspensions were used as seed cultures.

The sterilized-samples were placed in each vial containing 5 ml of LB medium and inoculated with 50 µl of seed culture. The cell suspension with the as-prepared BC was then incubated in a shaking incubator at 37°C for 24 h. After 24 h of incubation, each sample was diluted 10 times with saline then 50 µl of the suspension was dipped and spread on sterilized LB agar plates. Bacterial growth was visualized after an overnight incubation at 37°C. The counts of bacterial colonies were the surviving numbers of bacteria. The percent reduction in viable bacterial count was calculated by the formula:

$$\text{Percent reduction in viable cell count} = \frac{(Vcc_i - Vcc_f)}{Vcc_i} \times 100$$

Where Vcc_i: Viable cell count at 0 h.

Vcc_f: Viable cell count at 24 h.

6.4 Results and Discussion

In General, BC pellicle was produced in the form of hydrogel which exhibited high water content (98–99%), good sorption of liquids, high wet strength, and high chemical purity (Klemm, Schumann, Udhardt, & Marsch, 2001). The BC pellicle is constituted of multilayer structure of non woven network of nanofibrous cellulose. The unique nanometer scale structure of BC provides a large amount of hydroxyl groups on the pellicle surface. Therefore, the BC fibers exhibit super hydrophilic surface represented in the form of hydrogel or never-dried state. The never-dried state of BC provides a good tunnel for Zn^{2+} to penetrate through the BC matrix which corresponding to the concept of *in situ* synthesis. During the BC pellicle was immersed in the zinc acetate solution, Zn^{2+} was readily penetrated into the BC through their pores. Then, the penetrated-Zn^{2+} was trapped inside BC pellicle by bonding via electrostatic interactions with the electron-rich oxygen atoms of polar hydroxyl and ether groups at the surface of BC as shown in figure 6.1 (He, Kunitake, & Nakao, 2003). After immersion in zinc acetate solution, the Zn^{2+} absorbed-BC pellicle was then immersed in ammonium hydroxide solution (pH 8) and the ultrasonic treatment was simultaneously done. By reacting with the ammonium hydroxide, the absorbed-Zn^{2+} was converted to be ZnO inside the BC matrix according to the following reactions:

$$Zn^{2+}\,(aq) + 4NH_4OH\,(aq) \rightarrow (Zn(NH_3)_4)^{2+}\,(aq) + 4H_2O\text{-----(1)}$$

$$(Zn(NH_3)_4)^{2+}\,(aq) + 2OH^-\,(aq) + 3H_2O \rightarrow ZnO\,(s) + 4NH_4OH\,(aq)\text{-----(2)}$$

Scheme1 Synthesis route of ZnO by using Zn^{2+} as a precursor and NH_4OH as a catalyst (Perelshtein *et al.*, 2009).

Scheme1 shows synthesis route of ZnO particle by using Zn^{2-} as a precursor and NH_4OH as a catalyst. According to scheme1, the ammonium complex ($Zn(NH_3)_4^{2+}$) was formed via hydrolysis process of Zn^{2+} by using NH_4OH as catalyst. Then, the $Zn(NH_3)_4^{2+}$ was converted to ZnO by reacting with the hydroxyl groups (OH^-) under the extreme condition of ultrasonic treating (figure 6.1). Moreover, the ultrasonic treatment could also enhance the distribution of ZnO particle throughout the BC matrix. The well distribution of ZnO particle along the BC matrix was obtained as evidence by the original transparent and colorless of BC was turned to

the uniform white and opaque of BC pellicle. Finally, the as-prepared ZnO particle incorporated-BC pellicles were dried by freeze-drying method to maintain the original structure of BC (Klemm, Schumann, Udhardt, & Marsch, 2001).

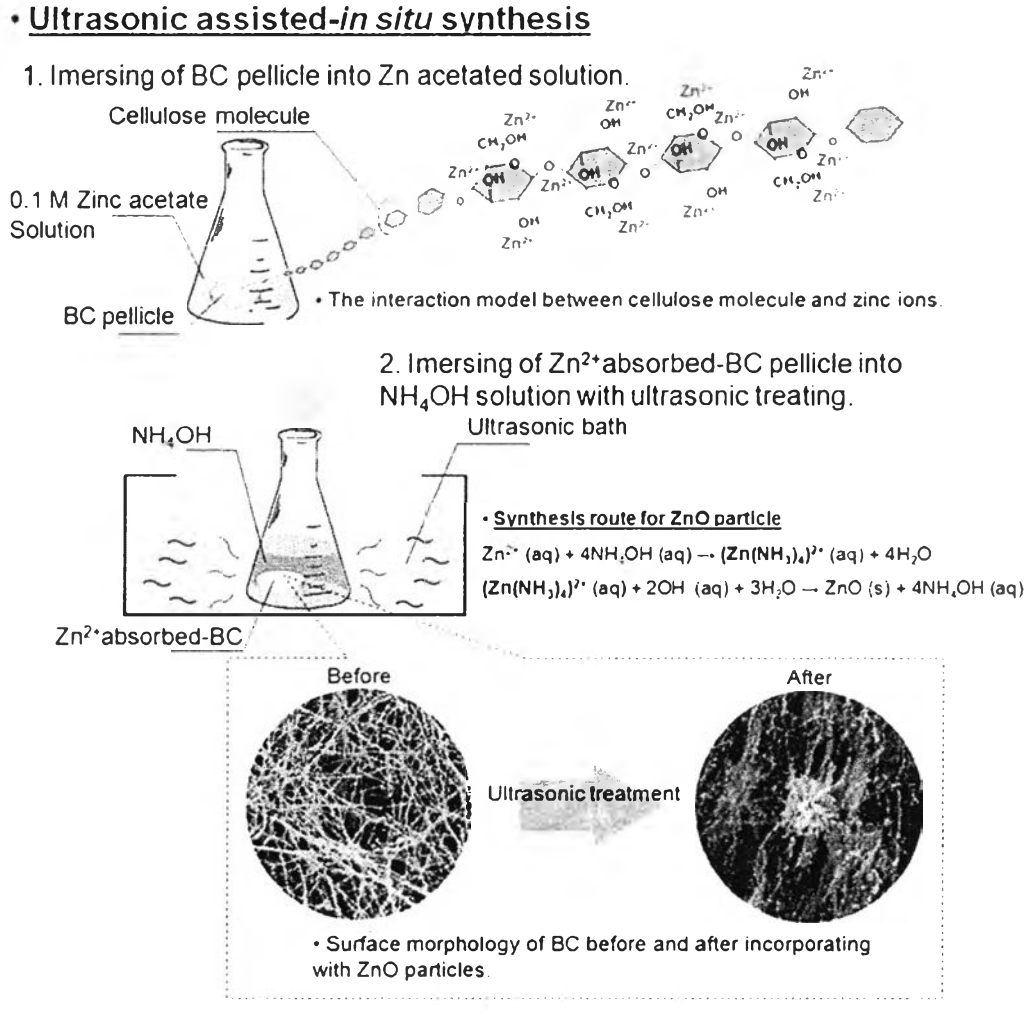

Figure 6.1 Schematic diagram of the experimental set-up for preparing of ZnO particle incorporated-BC by ultrasonic assisted-*in situ* synthesis method.

6.4.1 Morphology of the neat BC and the as-prepared ZnO particle incorporated-BC

The morphology of neat BC and the as-prepared ZnO particle incorporated-BC sample was investigated by the SEM. Figures 6.2a and b show the SEM images of surface and cross-sectional morphology of the neat BC at

magnification of 5,000× and 1500×, respectively. The surface morphology of neat BC exhibited the three-dimensional non-woven network structure of nanofibrous cellulose with a fiber diameter of 55.00 ±10.54 nm. Whereas the cross-sectional morphology of neat BC exhibited the multilayer structure of BC membranes linked together with the nano-fibrils. The multilayer structure of BC was resulted from the process of BC pellicle growth. The BC was firstly generated at the interface between air and the culture surface. As long as the system is kept unshaken, BC pellicle was generated a layer by layer slides steadily downwards as it thickens (Iguchi, Yamanaka, & Budhiono, 2000). This unique structure of neat BC was firmly supported the ultrasonic assisted-*in situ* synthesis method in that Zn^{2+} could simply incorporate throughout the BC matrix by simple immersion method. The hydrogel structure of BC pellicle provided good tunnels for Zn^{2+} adsorption resulted in the homogeneously distribution of Zn^{2+} inside the BC pellicle (Li, Chen, Hu, Shi, Shen, Zhang, & Wang, 2009). Then the absorbed Zn^{2+} was converted to ZnO by immersing the Zn^{2+} absorbed-BC pellicle into NH_4OH solution which simultaneously treated with the ultrasonic treatment. The formation of ZnO particles inside BC matrix was revealed by the SEM. Figures 6.2b and c show the SEM images of surface morphology of the as-prepared ZnO particle incorporated-BC sample prepared by the ultrasonic-assisted synthesis method with 6 h of immersion in zinc acetate solution and followed by 1 h of ultrasonic treatment at magnification of 650× and 5000×, respectively. The figures 6.2c and d show the surface morphology of non-woven network structure of BC with ZnO particles. The BC surface was expected to be a nucleating surface for ZnO crystal. By the aid of ultrasonic treatment, ZnO crystal was forced to growth perpendicular to the fiber surface and resembled to form a particle with size about 10 μm at the interconnecting point of BC fibrils (Figure 6.2d). The formation and distribution of ZnO particles inside BC were also verified by an elemental dot-mapping technique. Figures 6.2e and f show the X-ray dot mapping images for zinc elemental of the as-prepared ZnO particle incorporated-BC sample at magnification of 650× and 5000×, respectively. The positions of zinc element in the X-ray dot mapping images (figure 6.2e and f) were corresponded with the position of ZnO particle in the SEM images (figures 6.2c and d). These evidences clearly revealed the well-distribution of ZnO particles throughout the BC matrix.

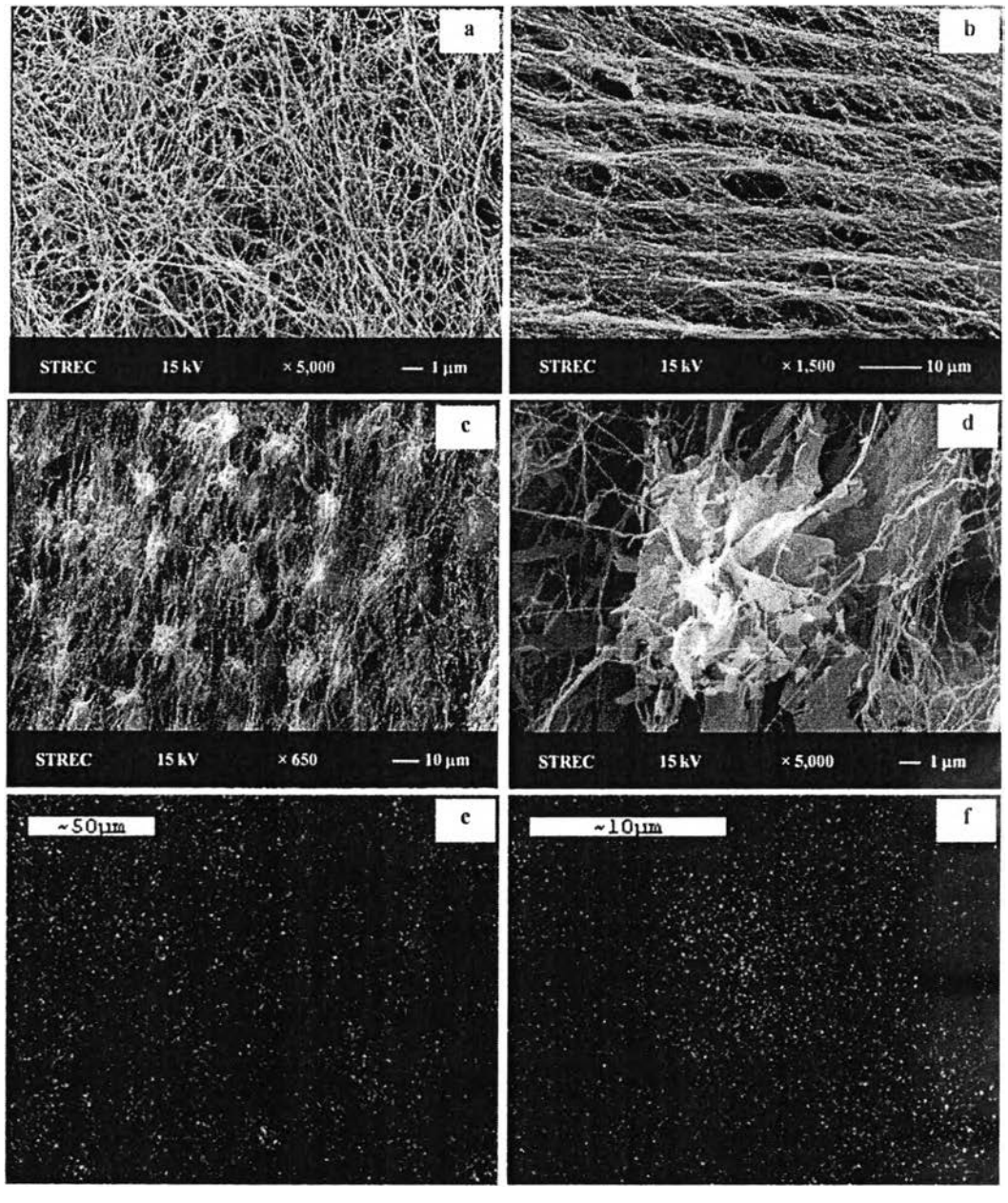

Figure 6.2 SEM images of surface and cross-sectional morphology of neat BC at magnification of 5,000× (a) and 1500× (b), respectively, SEM images of surface morphology of ZnO particle incorporated-BC prepared by the ultrasonic-assisted synthesis method with 6 h of immersion in zinc acetate solution and followed by 1 h of ultrasonic treatment at magnification of 650× (c) and 5,000× (d), respectively and X-ray dot mapping images for surface morphology of zinc elemental of ZnO particle incorporated-BC at magnification of 650× (e) and 5000× (f).

6.4.2 *The crystal structure and crystalline size of ZnO particles in the ZnO particle incorporated-BC*

The crystal structure of ZnO particles in the as-prepared ZnO particle incorporated-BC sample was investigated by the X-ray diffraction technique. Figure 6.3 shows the representative XRD spectra of the ZnO particle incorporated-BC prepared by the ultrasonic-assisted synthesis method with 6h (a), 3h (b) and 1h (c) immersing in zinc acetate solution and followed by 1h ultrasonic treating. All the XRD patterns of the as-prepared ZnO particle incorporated-BC sample showed the similar characteristic diffraction patterns with the similar characteristic diffraction peaks at 2θ = 31.7°, 34.4°, 36.2°, 47.5°, 56.6°, 62.8°, 66.4°, 67.9°, 69.1°,72.6° and 77.01°. These 11 characteristic diffraction peaks of ZnO particle incorporated BC were corresponded to (100), (002), (101), (102), (110), (103), (200), (112), (201), (004) and (202) planes, respectively. All these characteristic diffraction peaks indicated that the as-synthesized ZnO particles were hexagonal wurtzite structure (JCPDS Card, No 75-0576). According to the XRD pattern and SEM immages, there were clearly revealed that the ZnO particles was successfully incorporated into the nanofibrous matrix of BC by using ultrasonic assisted-*in situ* synthesis.

Moreover, the crystalline size of ZnO particles inside BC was also evaluated by the XRD diffraction peak. According to the Debye-Scherrer equation, the full width in the radians at a half-maximum (fwhm) of the X-ray diffraction peaks at the highest intensity peak (2θ = 36.3°) could be used for calculating the crystalline size of ZnO particles inside the as-prepared ZnO particle-incorporated BC sample. Table 1 showed crystalline sizes of ZnO particles inside the as-prepared ZnO particle incorporated-BC sample at various preparation conditions. The crystalline size of ZnO particles inside the as-prepared ZnO particle incorporated-BC sample prepared by ultrasonic assisted-*in situ* synthesis with 1 h, 3 h and 6h of immersion in zinc acetate solution and followed by 1 h of ultrasonic treatment were calculated to be 37.32 ±0.61 nm, 45.51 ±0.86 nm and 46.65 ±0.77 nm, respectively (table 1). The crystalline size of ZnO particles inside the as-prepared ZnO particle incorporated-BC sample was increased with increasing of the immersion of BC pellicle in zinc acetate solution. The increasing in the crystalline size of ZnO particles might result from the increasing in the percent incorporation of ZnO particle in the as-prepared ZnO

particle incorporated-BC (table 1). In order to investigate the effect of the ultrasonic treatment time on the crystalline size of ZnO particles, the immersion time of BC pellicle in zinc acetate solution was fixe at 3h and the ultrasonic treatment time was varied to be 0.5 h, 1 h and 2 h, respectively. The crystalline sizes of zinc oxide particles inside the as-prepared ZnO particle incorporated BC were decreased from 59.53 to 55.91 and to 53.83 nm with increasing the ultrasonic treatment time from 0.5 h to 1 h and to 2h, respectively (Table 1). The crystalline size of ZnO particles was decreased with increasing the ultrasonic treatment time. The decreasing of crystalline size of ZnO particles with increasing of the ultrasonic treatment time might result from the longer extreme condition treating by ultrasonic treatment, high temperature (>5000 K), pressure (>200 MPa), and cooling rates (>10^7 K/s), was reduced the crystalline size of the ZnO particle (Suslick, Choe, Cichowlas, & Grinstaff, 1991; Didenko, & Suslick, 2002). The advantage of BC matrix in the aspect of template for synthesizing of ZnO particles was investigated by comparing with other literatures. Perelshtein, Applerot, Perkas, Wehrschetz-Sigl, Hasmann, Guebitz, and Gedanken (2009) prepared nanocrystalline ZnO deposited-cotton bandage by using sonochemical irradiation process. The particle size of ZnO particle in nanocrystalline ZnO deposited-cotton bandage was increased from 30-400 nm with increasing the content of ZnO from 0.75-10.3 %wt, respectively. These results were corresponded to our results in that the crystalline size of was increased with the percent incorporating of ZnO particle in the as-prepared ZnO particle incorporated-BC. Anyways, almost of the literatures was used the sonochemical irradiation process as a method to coat or deposit the ZnO particle on the surface of matrix or polymer support (Kotlyar, Perkas, Amiryan, Meyer, Zimmermann, & Gedanken, 2007; Pol, Srivastava, Palchik, Palchik, Slifkin, Weiss, & Gedanken, 2002; Pol, Wildermuth, Felsche, Gedanken, & Calderon-Moreno, 2005). In this study, the incorporation of nanocrystalline ZnO particle through inside the BC matrix was firstly investigated by using the newly proposed-method that was called "ultrasonic assisted-*in situ* synthesis method". The nanocrystalline ZnO particles were successfully incorporated into the nanofibrous matrix of BC. By using the advantages of BC and the ultrasonic assisted-*in situ* synthesis method, the crystalline

size of nanocrystalline ZnO particle could be trailer made by adjusting the preparation conditions.

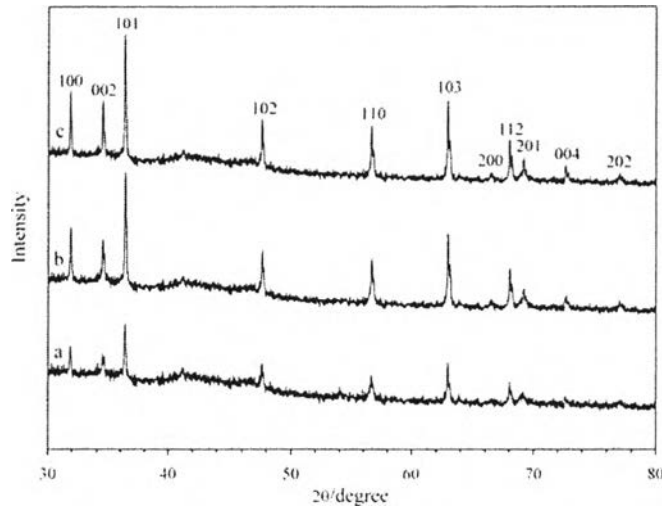

Figure 6.3 X-ray diffraction spectra of ZnO particle-incorporated BC prepared by ultrasonic-assisted synthesis method with 6h (a), 3h (b) and 1h (c) immersing in zinc acetate solution and followed by 1h ultrasonic treatment.

6.4.3 Thermal gravimetric analysis (TGA) of the as-prepared nanocrystalline ZnO particle incorporated-BC sample

The thermal stability of neat BC and the as-prepared ZnO particle incorporated-BC was studied by the TGA. In order to prevent the oxidation reaction between as-prepared samples and oxygen gas, all thermograms were recorded under the nitrogen atmosphere. The investigated temperature was ranged from 50°C to 750°C. Figures 6.4a and b show the TGA thermograms of the neat BC and the as-prepared ZnO particle incorporated-BC sample prepared by ultrasonic assisted-*in situ* synthesis method at various conditions. The thermograms of neat BC in the figures 6.4a and b show the main weight loss between 275 °C to 375 °C as a result of the thermal decomposition of BC. These include depolymerization, further dehydration, degradation of the glucopyranosyl units and subsequent oxidation leaving behind charred residues (Roman & Winter, 2004). Whereas, all of the thermograms of as-prepared ZnO particle incorporated-BC sample in the figures 6.4a and b exhibited the

similar pattern which composed of the two consecutive weight losses at 115°C and 200°C extending to 350°C. These two consecutive weight losses were corresponded to desorption of moisture and decomposition of BC, respectively (figure 6.4a and b). The degradation process of neat BC started at 275°C whereas the degradation process of the as-prepared ZnO particle incorporated-BC sample started at 200°C. The differences in onset thermal degradation temperature of BC between the neat BC and the as-prepared ZnO particle incorporated-BC sample might result from the lost of crystallinity of BC fibrils due to the ultrasonic treatment process.

Moreover, the percent incorporation of ZnO particles in the as-prepared ZnO particle-incorporated BC sample was also calculated by using TGA thermograms (Ghule *et al.*, 2006). The total weight loss of neat BC was 93.04 wt% and remaining 6.96 wt%. The remaining 6.96 wt% of percent weight loss could attribute to vestigial carbon of BC whereas the total weight losses of the as-prepared ZnO particle-incorporated BC sample prepared by immersing of BC pellicle in zinc acetate solution for 6, 3 and 1h and followed by 1h ultrasonic treatment were 43.79%, 51.73% and 52.89%, respectively (Figure 6.4a). The differences in weight losses between the neat BC and the as-prepared ZnO particle incorporated-BC sample were attributed to be the percent incorporation of ZnO particles in the as-prepared ZnO particle-incorporated BC sample. The percent incorporation of ZnO particles in all of the as-prepared ZnO particle-incorporated BC samples was also determined by the same manner. The test was repeated three times for each condition and summarized in table 1. The percent incorporation of ZnO particles in the as-prepared ZnO particle incorporated-BC sample prepared by immersing of BC pellicle in zinc acetate solution for 6, 3 and 1h and followed by 1h ultrasonic treatment were 37.32 ±0.61, 45.51 ±0.86 and 46.65 ±0.77 %wt, respectively. On the contrary, the percent incorporation of ZnO particles in the as-prepared ZnO particle incorporated-BC sample prepared by immersing of BC pellicle in zinc acetate solution for 3 and followed by 0.5, 1 and 2h of ultrasonic treatment were 44.27 ±0.50, 45.51 ±0.86 and 45.42 ±0.21%wt, respectively. These evidences indicated that BC pellicle was saturated with Zn^{2+} within 3 h of immersion (Figure 6.4a). In the other hand, the ultrasonic treatment time was a few affected on the percent incorporation of ZnO particles in the as-prepared ZnO particle incorporated-BC

sample. From these evidences, it can be elucidated that the immersion time of BC pellicle in zinc acetate solution had a major effect on the percent incorporation of ZnO particles in the as-prepared ZnO particle incorporated-BC sample. According to the advantages of BC matrix and ultrasonic assisted-*in situ* synthesis method, the ZnO particles were surprisingly preserved within the nanocrystalline size (63.25 nm) even at 46.65 ±0.77 %wt of ZnO particle. By using these aspects, the percent incorporation of ZnO particle in the as-prepared ZnO particle incorporated BC could be maximize with optimizing of the crystalline size of the incorporated-ZnO particles.

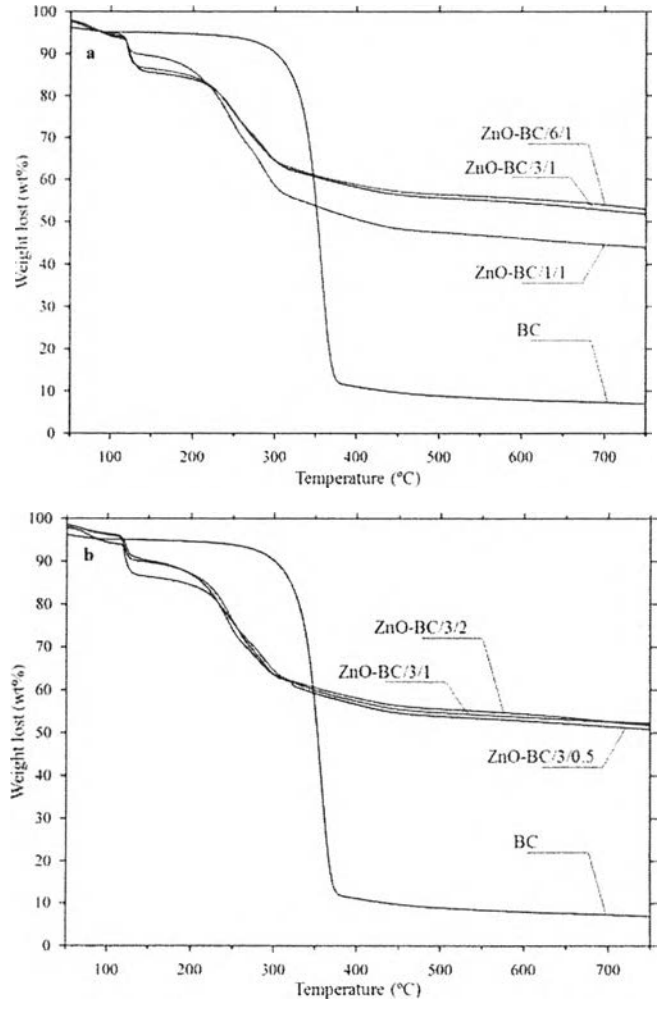

Figure 6.4 TGA thermograms of neat BC (BC) compared to that of nanocrystalline ZnO particle incorporated-BC were prepared by immersing of BC pellicle in zinc

acetate solution for 1 h (ZnO-BC/1/1), 3 h (ZnO-BC/3/1) and 6 h (ZnO-BC/6/1). Then, followed by 1 h of ultrasonic treatment time (a) and TGA thermograms of neat BC (BC) compared to nanocrystalline ZnO particle incorporated-BC prepared by immersing of BC pellicle in zinc acetate solution for 3 h and followed by 0.5 h (ZnO-BC/3/0.5), 1 h (ZnO-BC/3/1) and 2 h (ZnO-BC/3/2) of ultrasonic treatment time (b).

Table 6.1 Crystalline size and percent incorporation of ZnO particle inside the as-prepared ZnO particle incorporated-BC at various preparation conditions

Sample Ref.	Preparation condition		Crystalline size (nm)	Percent incorporation of ZnO (%wt)
	Immersion time (h)	Ultrasonic treatment time (h)		
ZnO-BC/6/1	1	1	54.70	37.32 ±0.61
ZnO-BC/3/1	3	1	55.91	45.51 ±0.86
ZnO-BC/1/1	6	1	63.25	46.65 ±0.77
ZnO-BC/3/0.5	3	0.5	59.53	44.27 ±0.50
ZnO-BC/3/1	3	1	55.91	45.51 ±0.86
ZnO-BC/3/2	3	2	53.83	45.42 ±0.21

*ZnO-BC/x/y: ZnO particle incorporated-BC/Immersion time of BC pellicle in zinc acetate solution (h)/ Ultrasonic treatment time (h)

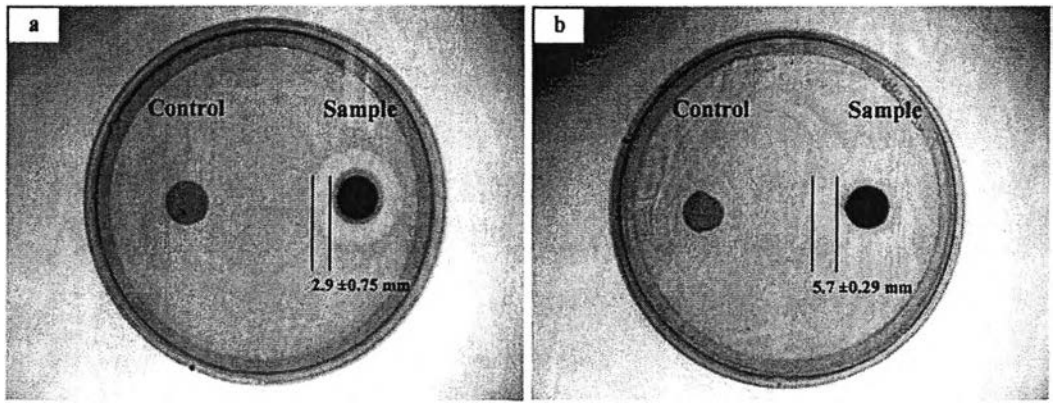

Figure 6.5 Antibacterial activity of as-prepared ZnO particle incorporated-BC sample with 37.32 ±0.61 %wt of ZnO against (a) *S. aureus* and (b) *E. coli*.

6.4.4 Antibacterial activity of the as-prepared ZnO particle incorporated-BC sample

In order to investigate the unique properties of nanocrystalline ZnO particles in the as-prepared ZnO particle-incorporated BC sample, the antibacterial activities of the as-prepared ZnO particle-incorporated BC sample were desired to be a representative study. The antibacterial activities of the as-prepared ZnO particle incorporated-BC sample were studied by using the disc diffusion method and the colony forming count method. *S. aureus* and *E. coli* were selected as a model of gram-negative and gram-positive bacteria, respectively.

6.4.4.1 The disc diffusion method

The disc diffusion method is a qualitative method for roughly determining the antibacterial activity of the as-prepared ZnO particle incorporated-BC sample. The disc diffusion method was performed by monitoring the visualized inhibition ring of the sample on the solid agar culture plate. In these tests, the neat BC and the as-prepared ZnO particle incorporated-BC were placed on *E. coli*-cultured agar plates and *S. aureus*-cultured agar plates which were then incubated at 37°C for 24 h. Figure 6.5 showed the antibacterial activity of the as-prepared ZnO particle incorporated-BC sample with 37.32 ±0.61 %wt of ZnO against *S. aureus* (a) and *E. coli* (b). After 24 h-incubation at 37°C, the growth of

bacteria on solid agar culture plate was visualized in both *E. coli*-cultured agar plates and *S. aureus*-cultured agar plates. The clear zone with no bacterial growth was observed as an inhibition ring around the as-prepared ZnO particle incorporatted-BC sample. The thickness of inhibition ring for *S. aureus* and *E. coli* were 2.9 ±0.75 and 5.7 ±0.29 mm, respectively and no inhibition ring was observed with neat BC (figure 6.5). These could reveal that the antibacterial activity of the as-prepared ZnO particle incorporated-BC sample was resulted from the incorporated-nanocrystalline ZnO particles and the nanocrystalline ZnO particles were also exhibited the unique antibacterial activity even incorporating inside BC matrix. Moreove, the antibacterial activity of as-prepared ZnO particle incorporated-BC sample was exhibited the significantly difference against two strains of bacteria. In that *E. coli* were more susceptible to the antibacterial activity of nanocrystalline ZnO particle than *S. aureus*, these could be explained by the difference in their sensitivity toward the oxy-radicals which were generated by reaction between ZnO particles and water by using visible light as a catalyst. *S. aureus* bacteria contained a large amount of cartenoid pigment, which promotes higher resistance to oxidative stress (Liu, Essex, Buchanan, Datta, Hoffman, Bastian, Fierer & Nizet, 2005).

6.4.4.2 The colony forming count method

The colony forming count method is a quantitative method for determining the antibacterial activity of the as-prepared ZnO particle incorporated-BC sample. The colony forming count method was performed by incubating of sample with the bacteria cell in liquid culture media for 24 h at 37°C. Then, the 24 h-incubated liquid culture media was diluted and sampled for monitoring the numbers of viable bacteria cell. The numbers of viable bacteria cells were reported in the term of colony-forming unit/ml of liquid culture media (CFU/ml). The numbers of viable bacteria cell before and after incubation with the as-prepared ZnO particle incorporated-BC sample were shown in Table 2. For the as-prepared ZnO particle incorporated-BC sample with 37.32 ±0.61 %wt of ZnO, the number of viable cell of *E. coli* and *S. aureus* bacteria was decreased from 3.4×10^7 and 2.4×10^7 CFU/ml to 6.8×10^4 $\pm1.02\times10^4$ and 4.9×10^4 $\pm0.5\times10^4$ CFU/ml, respectively. The percent reduction in viable cell of *E. coli* and *S. aureus* bacteria for

the as-prepared ZnO particle incorporated-BC sample with 37.32 ±0.61 %wt of ZnO was calculated to be 99.8 ±0.02% and 99.8 ±0.03%, respectively. For the neat BC, the number of viable cell of *E. coli* and *S. aureus* bacteria was increased from 3.4×10^7 and 2.4×10^7 CFU/ml to 4.6×10^7 $\pm5.2\times10^4$ and 3.5×10^7 $\pm6.4\times10^4$ CFU/ml, respectively. The percent reduction in viable cell of *E. coli* and *S. aureus* bacteria for the neat BC was calculated to be -34.1 ±0.15%and -45.2 ±0.26%, respectively. The percent reduction in viable cell of *E. coli* and *S. aureus* bacteria for the as-prepared ZnO particle incorporated-BC sample with 45.51 ±0.86 and 46.65 ±0.77 %wt was summarized in table 2. All the as-prepared ZnO particle incorporated-BC samples were exhibited the promising antibacterial activity with approximately 99.8 % reduction in cell viability. The strong antimicrobial activity of the as-prepared ZnO particle incorporated-BC sample might result from it porous structure. This structure provided the empty space for allowing the water molecule to react with the ZnO particle for generating the reactive species such as oxy-radical or hydroxyl-radical. These reactive species could oxidative injury inside bacteria cell resulting in the strong antibacterial property of the as-prepared ZnO particle incorporated-BC sample. All these evidences were confirmed that the nanocrystalline ZnO particles were successfully synthesizing and simultaneously incorporation into nanofibrous matrix of BC by using the ultrasonic assisted-*in situ* synthesis method.

Table 6.2 Colony forming unit counts (CFU/ml) at 0h and 24h contact time intervals with the as-prepared ZnO particle incorporated-BC against *S. aureus* and *E. coli*

Samples Reference	Percent incorporation of ZnO (%wt)	*E. coli* (CFU/ml)			*S. aureus* (CFU/ml)		
		Contact time		% Reduction in cell viability	Contact time		% Reduction in cell viability
		0 h	24 h		0 h	24 h	
BC	0	3.4×10^{7}	$4.6\times10^{7}(\pm5.2\times10^{4})$	-34.1 ±0.15%	2.4×10^{7}	$3.5\times10^{7}(\pm6.4\times10^{4})$	-45.2 ±0.26%
ZnO-BC	37.32 ±0.61	3.4×10^{7}	$6.8\times10^{4}(\pm1.02\times10^{4})$	99.8 ±0.02%	2.4×10^{7}	$4.9\times10^{4}(\pm0.5\times10^{4})$	99.8 ±0.03%
	45.51 ±0.86	3.4×10^{7}	$7.0\times10^{4}(\pm0.52\times10^{4})$	99.79 ±0.02%	2.4×10^{7}	$5.04\times10^{4}(\pm0.48\times10^{4})$	99.79 ±0.02%
	46.65 ±0.77	3.4×10^{7}	$6.8\times10^{4}(\pm0.9\times10^{4})$	99.79 ±0.03%	2.4×10^{7}	$5.04\times10^{4}(\pm0.72\times10^{4})$	99.8 ±0.03%

BC: Neat BC

ZnO-BC: ZnO particle incorporated-BC

6.5 Conclusions

In this study, nanocrystalline ZnO particles were successfully synthesized and incorporated into nanofibrous matrix of BC by using the ultrasonic assisted-*in situ* synthesis method. The new proposed- preparation method was surprisingly simple and easy which composed of the two step-wised immersion methods. Briefly, BC pellicle was firstly immersed in zinc acetated solution. Then, the Zn^{2+} absorbed-BC pellicle was immersed in ammonium hydroxide solution and simultaneously treating with the ultrasonic treatment. By applying the ultrasonic treatment, the nanocrystalline ZnO particles were forced to growth inside the BC matrix by using the surface of nanofibrous BC as a nucleating agent for ZnO crystal. Then, the ZnO crystals were growth and formed to be a nanocrystalline ZnO particle inside the BC matrix. The SEM and EDX images were clearly revealed the formation of the as-prepared nanocrystalline ZnO particles inside the BC matrix. The multilayer structure of three-dimensional nonwoven network of nanofibrous BC was acted as the promising template for synthesizing of the nanocrystalline ZnO particles. The as-prepared nanocrystalline ZnO particles inside BC matrix were represented in the form of the hexagonal wurtzite structure with the average crystalline size of 57.19 ±3.55 nm. The average crystalline size of nanocrystalline ZnO particles inside the as-prepared nanocrystalline ZnO particle-incorporated BC sample were corresponded to the average fiber diameter of the nanofibrous BC (44.46–65.54 nm). The average crystalline size of ZnO particles inside the as-prepared nanocrystalline ZnO particle-incorporated BC sample were significantly increased with increasing the immersion time of BC pellicle in the zinc acetate solution. The increasing in the crystalline size of ZnO particles with increasing the immersion time was resulted from the increasing in the percent incorporation of ZnO particles inside the as-prepared nanocrystalline ZnO particle incorporated-BC sample while providing a longer immersion time of BC pellicle in zinc acetate solution. The percent incorporation of nanocrystalline ZnO particles were increased from 36.82 to 44.77 wt% with increasing the immersion time of BC pellicle in zinc acetate solution from 1 to 3 h then the percent incorporation of nanocrystalline ZnO particles was reached to the equilibrium at 45.93 wt% with 6 h of the immersion time. Interestingly, the crystalline size of ZnO

particles was still in the range of nanometer scale even at a high percent incorporation of ZnO particle (45.93 wt%). By using BC as a template for synthesizing of ZnO particles, the crystalline sizes of ZnO particles were controlled in the range of nanometer scale. These evidences could support the advantages of BC matrix in the aspect of template for synthesizing of the nanocrystalline ZnO particles. The antibacterial activity of the as-prepared nanocrystalline ZnO particle incorporated-BC were investigated in order to confirm the unique properties of the nanocrystalline ZnO paticles inside the as-prepared nanocrystalline ZnO particle incorporated-BC. The freeze-dried nanocrystalline ZnO particle-incorporated BC exhibited the 99.8 % reduction in viable cell of *E. coli* (Gram-negative bacteria) and *S. aureus* (Gram-positive bacteria). This could verify the antibacterial activity of the as-prepared nanocrystalline ZnO particle-incorporated BC in that the incorporated-nanocrystalline ZnO particles were still exhibited strong antibacterial activity against board spectrum of bacteria even incorporating into the BC matrix. In summarized, the ultrasonic assisted-*in situ* synthesis method was one of the effective preparation methods for incorporating of the nanocrystalline ZnO particles into nanofibrous matrix of BC. The unique morphology of nanofibrous BC provided the nanometer scaled-surface for supporting the crystal of ZnO. Therefore, the crystalline size of the incorporated-ZnO particles were in the ranged of nanometer scale even at high percent incorporation of ZnO particles in the BC matrix. According to the advantages of preparation method and BC matrix, the as-prepared nanocrystalline ZnO particle incorporated-BC was exhibited the strong antibacterial activity against *E. coli* (Gram-negative) and *S. aureus* (Gram-positive). Moreover, the preparation method was simple, cost-effective and environmental friendly, which may provide a facile approach toward the manufacturing of metal oxide nanocomposites, antimicrobial materials, low-temperature catalysts and other useful materials. By using this preparation method, the antibacterial properties also could be achieved into the other materials such as electro-spun nanofiber mat and other porous materials.

6.6 Acknowledgements

This work is greatly supported in cash and in kind by the Chulalongkorn University Dutsadi Phiphat Scholarship, The Petroleum and Petrochemical College, Chulalongkorn University, Center of Excellence on Petrochemical and Materials Technology and Kansai University, Japan, are greatly acknowledged.

6.7 References

An, X., Cao, C., & Zhu, H. (2007). Bio-inspired fabrication of ZnO nanorod arrays and their optical and photoresponse properties. *Journal of Crystal Growth, 308(2)*, 340–347.

Applerot, G., Perkas, N., Amirian, G., Girshevitz, O., & Gedanken, A. (2009). Coating of glass with ZnO via ultrasonic irradiation and a study of its antibacterial properties. *Applied Surface Science, 256S*, S3–S8.

Applerot, G., Lipovsky, A., Dror, R., Perkas, N., Nitzan, Y., Lubart, R., & Gedanken, R. (2009). Enhanced Antibacterial Activity of Nanocrystalline ZnO Due to Increased ROS-Mediated Cell Injury. *Advanced Functional Materials, 19*, 842–852.

Cao, X., Lan, X., Zhao, C., Shen, W., & Yao, D. (2008). Porous ZnS/ZnO microspheres prepared through the spontaneous organization of nanoparticles and their application as supports of holding CdTe quantum dots. *Materials Research Bulletin, 43(5)*, 1135–1144.

Casavola, M., Buonsanti, R., Caputo, G., & Cozzoli, P.D. (2008). Colloidal Strategies for Preparing Oxide-Based Hybrid Nanocrystals. *European Journal of Inorganic Chemistry*, 6, 837–854.

Czaja, W. K., Romanovicz, D., & Brown, R. M., (2004). Structural investigations of microbial cellulose produced in stationary and agitated culture. *Cellulose, 11*, 403–411.

Czaja, W. K., Young, D. J., Kawecki, M., & Brown, R. M. (2007). The future prospects of microbial cellulose in biomedical applications. *Biomacromolecules, 8*, 1–12.

Didenko, Y., & Suslick, K. S. (2002). The Energy Efficiency of Formation of Photons, Radicals, and Ions During Single Bubble Cavitation. *Nature, 418*, 394–397.

Dubey, V., Saxena, C., Singh, L., Ramana, K. V., & Chauhan R. S. (2002) Pervaporation of binary water–ethanol mixtures through bacterial cellulose membrane. *Separation and Purification Technology, 27*, 163–171.

Ghule, K., Ghule, A. V., Chen B., & Ling, Y. (2006). Preparation and characterization of ZnO nanoparticles coated paper and its antibacterial activity study. *Green Chemistry, 8*, 1034–1041.

Grzegorczyn, S., & Ezak, A. (2007). Kinetics of concentration boundary layers buildup in the system consisted of microbial cellulose biomembrane and electrolyte solutions. *Journal of Membrane Science, 304*, 148–155.

He, J., Kunitake, T., & Nakao, A. (2003). Facile in situ synthesis of noble metal nanoparticles in porous cellulose fibers. *Chemistry of Materials, 15*, 4401–4406.

Hirai, T. & Asada, Y., (2005) Preparation of ZnO nanoparticles in a reverse micellar system and their photoluminescence properties. *Journal of Colloid and Interface Science, 284*, 184–189.

Hu, W., Chen, S., Li, X., Shi, S., Shen, W., Zhang, X., & Wang, H. (2009). In situ synthesis of silver chloride nanoparticles into bacterial cellulose membranes. *Materials Science and Engineering C, 29*, 1216–1219.

Hu, W., Chen, S., Zhou, B., & Wang, H. (2010). Facile synthesis of ZnO nanoparticles based on bacterial cellulose. *Materials Science and Engineering B, 170*, 88–92.

Iguchi, M., Yamanaka, S., & Budhiono, A. (2000). Bacterial cellulose–A masterpiece of nature's arts. *Journal of Materials Science, 35(2)*, 261–270.

Jia, Z., Yue, L., Zheng, Y., & Xu, Z. (2008). Rod-like zinc oxide constructed by nanoparticles: synthesis, characterization and optical properties. *Materials Chemistry and Physics, 107(1)*, 137–141.

Jung, S., Oh, E., Lee, K., Yang, Y., Park, C., Park, W. & Jeong, S (2008). Sonochemical Preparation of Shape-Selective ZnO Nanostructures. *Crystal growth & design*, 8(1), 265–269.

Kamel, S. (2007). Nanotechnology and its applications in lignocellulosic composites, a mini review. *eXPRESS Polymer Letters, 1*, 546–575.

Klemm, D., Schumann, D., Udhardt, U., & Marsch, S. (2001). Bacterial synthesized cellulose-artificial blood vessels for microsurgery. *Progress in Polymer Science, 26(9)*, 1561–1603.

Kotlyar, A., Perkas, N., Amiryan, G., Meyer, M., Zimmermann, W., & Gedanken, A. (2007). Coating silver nanoparticles on poly(methyl methacrylate) chips and spheres via ultrasound irradiation. *Journal of Applied Polymer Science, 104(5)*, 2868–2876.

Lee, J.H., Ko, K.H. & Park. B.O. (2003). Electrical and optical properties of ZnO transparent conducting films by the sol–gel method. *Journal of Crystal Growth*, 247, 119–125.

Li, C., Fang, G., Liu, N., Ren, Y., Huang, H., & Zhao, X. (2008). Snowflake-like ZnO structures: self-assembled growth and characterization. *Materials Letters, 62(12–13)*, 1761–1764.

Li, X., Chen, S., Hu, W., Shi, S., Shen, W., Zhang, X. & Wang H. (2009). In situ synthesis of CdS nanoparticles on bacterial cellulose nanofibers. *Carbohydrate Polymers, 76*, 509–512.

Liu, G.Y., Essex, A., Buchanan, J.T., Datta, V., Hoffman, H.M., Bastian, J.F., Fierer, J., & Nizet, V. (2005) *Staphylococcus aureus* golden pigment impairs neutrophil killing and promotes virulence through its antioxidant activity. *Journal of Experimental Medicine, 202*, 209–215.

Liu, J., Huang, X., Li, Y., Duan, J., & Ai, H. (2006) Large-scale synthesis of flower-like ZnO structures by a surfactantfree and low-temperature process. *Materials Chemistry and Physics, 98(2–3)*, 523–527.

Maneerung, T., Tokura, S., & Rujiravanit, R. (2008). Impregnation of silver nanoparticles into bacterial cellulose for antimicrobial wound dressing. *Carbohydrate Polymers, 72*, 43–51.

Perelshtein, I., Applerot, G., Perkas, N., Wehrschetz-Sigl, E., Hasmann, A., Guebitz, G.M. & Gedanken, A. (2009). Antibacterial Properties of an *In Situ* Generated and Simultaneously Deposited Nanocrystalline ZnO on Fabrics. *ACS Applied Materials and Interfaces, 1(2)*, 361–366.

Pol, V. G., Srivastava, D. N., Palchik, O., Palchik, V., Slifkin, M. A., Weiss, A. M., & Gedanken, A. (2002). Sonochemical Deposition of Silver Nanoparticles on Silica Spheres. *Langmuir, 18*, 3352–3357.

Pol, V. G., Wildermuth, G., Felsche, J., Gedanken, A., & Calderon-Moreno, J. (2005). Sonochemical Deposition of Au Nanoparticles on Titania and the Significant Decrease in the Melting Point of Gold. *Journal of Nanoscience and Nanotechnology, 5 (6)*, 975–979.

Rezaee, A., Solimani, S., & Forozandemogadam, M. (2005). Role ofplasmid in production of Acetobacter xylinum biofilms. *American Journal of Biochemistry and Biotechnology, 1*, 121–125.

Roman, M., & Winter, W. T. (2004) Effect of sulfate groups from sulfuric acid hydrolysis on the thermal degradation behavior of bacterial cellulose. *Biomacromolecules, 5*, 1671–1677.

Sue, K., Kimura, K., & Arai. K. (2004). Hydrothermal synthesis of ZnO nanocrystals using microreactor, *Materials Letters*, 58, 3229–3231.

Sulieman, K. M., Huang, X., Liu, J., & Tang, M. (2007). Formation of ZnO three-side teethed nanostructures. *Materials Letters*, *61(8–9)*, 1756–1759.

Suslick, K. S., Choe, S. B., Cichowlas, A. A., & Grinstaff, M. W. (1991). Sonochemical synthesis of amorphous iron. *Nature, 353*, 414–416.

Tani, T., Madler, L., and Pratsinis.S.E. (2002). Homogeneous ZnO Nanoparticles by Flame Spray Pyrolysis, *Journal of nanoparticle research*, 4(4), 337–343.

Wan, Y., Hong, L., Jia, S., Huang, Y., Zhu, Y., Wang, Y., & Jiang, H. (2006). Synthesis and characterization of hydroxyapatite-bacterial cellulose nanocomposites. *Composites Science and Technology, 66*, 1825–1832.

Wang, L. N. & Muhammed. M. (1999). Synthesis of zinc oxide nanoparticles with controlled morphology. *Journal of Materials Chemistry*, 9, 2871-2878.

Wu, J. J., & Liu, S. C. (2002). Catalyst-free growth and characterization of ZnO nanorods. *Journal of Physical Chemistry B, 106(37)*, 9546–9551.

Wu, L., Wu, Y., & Lü, Y. (2006). Self-assembly of small ZnO nanoparticles toward flake-like single crystals. *Materials Research Bulletin*, *41(1)*, 128–133.

Wu, J. J. & Liu. S.S. (2002). Catalyst-Free Growth and Characterization of ZnO Nanorods. *The Journal of Physical Chemistry B*, 106 (37), 9546–9551.

Zhang, D., & Qi, L. (2005). Synthesis of mesoporous titania networks consisting of anatase nanowires by templating of bacterial cellulose membranes. *Chemical Communications, 21*, 2735–2737.